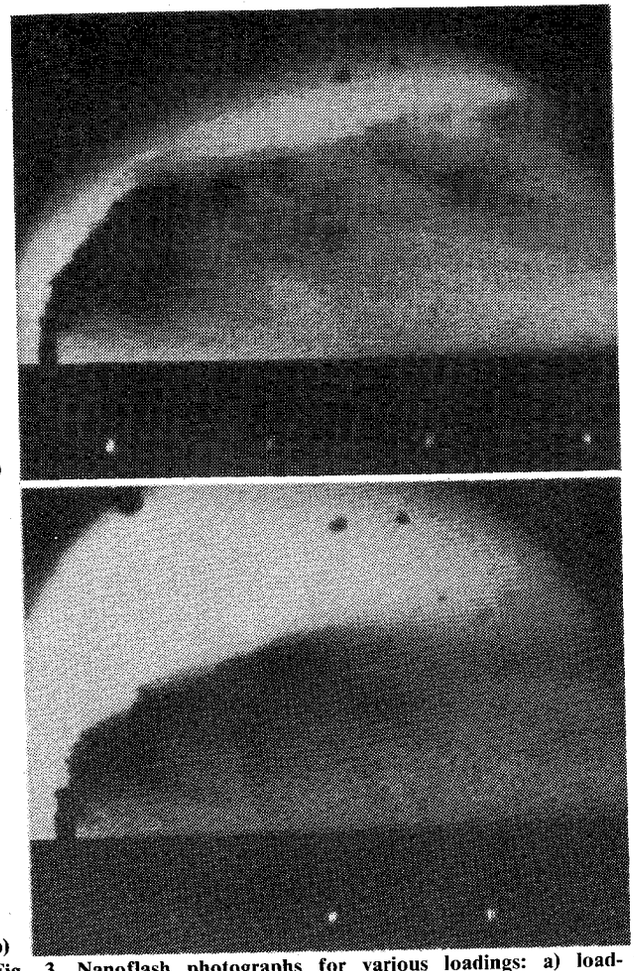

Fig. 3 Nanoflash photographs for various loadings: a) loading = 16%, $\bar{q} = 4.2$; b) loading = 52%, $\bar{q} = 4.2$.

creased, the penetration decreases. This latter relationship can be attributed to the combined factors of particle/liquid interactions and the definition of $\bar{q}$ for slurries. The momentum flux ratio $\bar{q}$ depends explicitly on the density of the slurry. This dependence upon the density is noteworthy since two jets with the same $\bar{q}$ but with different loadings (densities) will possess different jet velocities.

Further studies of the penetration were performed by light extinction methods. An all-liquid jet and a slurry jet of 40% loading were surveyed. The momentum flux ratio of both jets was 7.0. A transverse survey of each jet was performed at a location 30 mm downstream of the orifice.

In Fig. 1, it can be seen that the liquid jet penetrated further and had a higher extinction than the slurry jet. Furthermore, the extinction profiles for the two jets are similar except for the slopes on the upward part of the jets. The all-liquid jet has a slightly steeper slope (i.e., the extinction decreased more rapidly), which corresponds to a sharper penetration profile on the streak pictures.

The extinction experiments also raised some questions concerning the definition of penetration. The penetration as measured from the streak photographs is marked on Fig. 1 for both jets. Based on the extinction curves, the penetration height found from the streak photographs does not correspond directly to any physical phenomenon. However, since the penetration heights presented in this and other reports are primarily for comparison purposes only, the ambiguity about the penetration height does not adversely affect the stated results.

Jet Breakup

The breakup process of the slurry jet was noticeably less violent than its all-liquid counterpart. The lessening of the violence can be seen in the raw data for the extinction tests which consisted of the time variation of the undiffracted beam intensity. Both of the jets showed unsteadiness in the curves, as is evident in the sample curves presented in Fig. 2. The amplitudes of the fluctuations for the slurry jet are dramatically less than those for the all-liquid jet. Examination of the nanoflash pictures suggests that the slurry jets do indeed become more steady as the loading is increased. Compare the jets depicted in Fig. 3.

The maximum amplitudes in the fluctuations occurred 3 mm above the point of maximum extinction for each jet. The maximum amplitudes, in terms of the streak photographs, occurred at the penetration height of each jet.

Phase Separation

From the nanoflash photographs, the particles are shown to penetrate 40-45% farther into the airstream than the liquid portion of the jet. The particles that separated were actually agglomerates of particles. These clumps were 25-40 μm in diameter. The particles agglomerated or flocculated due to the interparticle attraction of small wetted particles. Smaller agglomerates can be seen within the liquid plume.

Water was contained within the separated agglomerates. In several nanoflash pictures, water can be seen being sheared away from the particles. The shearing is visible in the comet-like structures: the "head" of the comet is the agglomerate and the "tail" is formed by the water as it was being sheared away.

Conclusions

The behavior of the agglomerated particles found can be compared with the behavior of particles in particle-laden gas jets. Small clumps remain within the confines of the liquid jet, but are shifted toward separation. Clumps with diameters greater than 25 μm separate from the jet, following paths dictated by their mass and momentum. About one-eighth of the particles separate, and they penetrate up to 45% further into the cross stream than the liquid phase.

The separation of the phases results in reduced penetration of the liquid portion of the injectant as the loading is increased.

The slurry jets are more stable than all-liquid jets. In the present study, the stability was noted as a decrease in fluctuations in the jet.

Acknowledgment

This work was supported by the U.S. Air Force Office of Scientific Research; B.T. Wolfson was the Project Monitor.

Further Experiments on Shock Tube Wall Boundary-Layer Transition

Michael J. Chaney* and William J. Cook†
Iowa State University, Ames, Iowa

Nomenclature

M = Mach number
p = pressure
Re_T = $\rho_2 U_2 X_T / \mu_2$, transition Reynolds number

Received April 12, 1982; revision received Oct. 18, 1982.

*Graduate Student; presently Project Engineer, Sverdrup Technology, Inc., AEDC Group, Arnold Air Force Station, Tenn.
†Professor, Mechanical Engineering Department. Member AIAA.

Re_u = unit Reynolds number, m^{-1}
T = temperature
t_T = transition time (time from shock arrival to transition front arrival at a given location)
U = velocity
X_T = $U_2 U_s t_T / U_e$, characteristic length
μ = dynamic viscosity
ρ = density

Subscripts

1 = condition downstream of shock in laboratory coordinates
2 = condition in uniform flow region upstream of shock in laboratory coordinates
e = condition in freestream in shock-fixed coordinates
s = pertains to moving shock wave in laboratory coordinates
w = condition at the wall

Introduction

REGARDING laminar-to-turbulent transition in unsteady shock-tube wall boundary layers, there are numerous reports (e.g., Refs. 1 and 2) supporting the concept that environmental disturbances cause transition to occur in a Reynolds number regime where the laminar boundary layer is theoretically stable. In this Note, experimental data are presented from an investigation of the effects on transition of environmental disturbances which originate during the shock-tube driving process. Also reported are measured transition Reynolds numbers which are larger than previously published data for the range of wall cooling covered in the present study.

The shock-tube disturbance environment is characterized by freestream vorticity or roughness-caused turbulence and acoustic radiation. Disturbances produced by turbulent mixing at the contact surface and noise from the turbulent wall boundary layer propagate downstream toward the developing laminar boundary layer. To these sources of disturbances, however, should be added the shock-tube driving process. When a diaphragm is burst to initiate flow, the expanding driver gas and the ruptured diaphragm cause shock-tube recoil, acoustic noise, and structural vibrations. These "driver-created" disturbances precede the development of the other disturbances described above. Therefore, the variables which dictate the characteristics of driver-created disturbances (driver gas, driver pressure, and diaphragm) could influence the disturbances which impinge on the laminar boundary layer and affect transition behavior. Boison,[3] using microphones and accelerometers to measure shock-tube disturbances, correlated disturbance measurements with wall boundary-layer transition data. One conclusion was that transition behavior was unaffected by driver or diaphragm characteristics. However, this conclusion was not derived entirely from isolating the effects of driver-created disturbances during the experiments. Instead, it was partially based on agreement with other published transition data.

In the present investigation, a systematic approach was applied to study the effect of driver-created disturbances. Experiments were conducted at a fixed test condition with a given shock Mach number and initial test section pressure to produce a controlled wall boundary layer. Driver-created disturbances were varied by testing with three different driver gases. Due to differences in the thermodynamic properties of the gases, each required different driver pressure and diaphragm thickness. These driver parameters dictate the levels of recoil, noise, and vibration, with the driver pressure being the major contributor. With the test condition fixed, the only source of variation in the disturbance environment resulted from the driver-created disturbances associated with the three driver gases.

Table 1 Driver conditions

Driver gas	Driver gage pressure, kPa	Mylar diaphragm thickness, mm
50% helium, 50% air[a]	200	0.127
Air	6,300	0.305
Carbon dioxide	11,000	0.457

[a] Mole fraction.

Experiments

The cold gas driven shock tube used in the present study was constructed of extruded 6061-T6 aluminum with square cross section and internal dimensions of 12.7×12.7 cm. This material provided smooth, uniform wall surfaces. Two carefully hand-finished joints, located 3.96 and 4.57 m from the diaphragm, were upstream of the 3.96 m long test section. Thin-film heat gages mounted flush on the centerline of the vertical walls were used to detect boundary-layer transition. Typically, four gages mounted at different axial locations in the test section were monitored simultaneously. Test time in the uniform flow region was measured with a constant temperature hot-wire anemometer or a fast-response stagnation pressure probe. All data were recorded photographically on oscilloscopes.

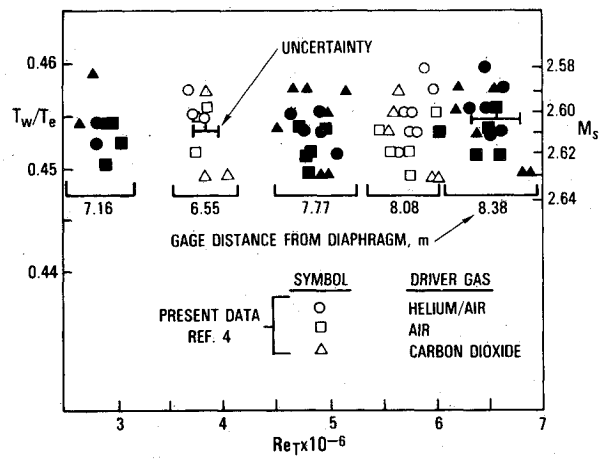

Fig. 1 Transition Reynolds numbers for three driver gases.

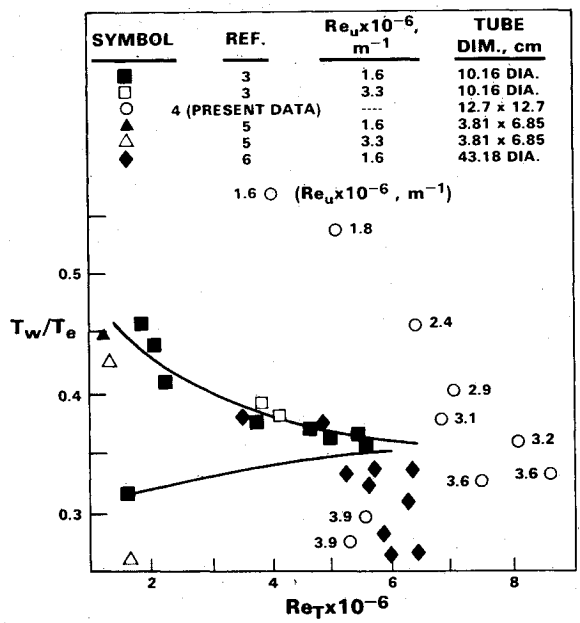

Fig. 2 Comparison of transition data for similar unit Reynolds numbers.

These experiments were conducted at a nominal condition of $M_s = 2.60$, $Re_u = 2.4 \times 10^6$/m, and $p_1 = 2.933$ kPa with air as the driven gas. In Table 1, driver conditions are listed for the three driver gases. Since driver-created disturbances depend primarily on driver pressure, carbon dioxide produced the most violent disturbances. Measurements of the disturbance environment for correlation to transition data were not obtained.

Results

Transition Reynolds number results from tests at the nominal test condition are presented in Fig. 1 for each driver gas. Data at shock Mach numbers of 2.58-2.63 are included. At each gage location, the data are identified by alternate solid and open symbols and by brackets. Note that the data fall within definite bounds at each gage, indicating no trend in Re_T due to driver gas. Thus, while shock-tube recoil, noise, and vibration disturbances varied according to driver conditions, there was no observed influence of driver-created disturbances on boundary-layer transition. This result is in agreement with Boison's conclusion.[3] For this series of tests, 14% of the data were anomalous, with Re_T values lying both above and below the distinct ranges for each gage in Fig. 1. Nonetheless, these outliers also showed no influence of driver-created disturbances. Another anomaly appears in Fig. 1, namely that Re_T at 6.55 m is larger than at 7.16 m. Such a result is contrary to the transition front concept. For the usual case of approximately constant transition front velocity with a magnitude less than U_s, the expected result would be higher Re_T at 7.16 m. This anomaly was thoroughly investigated, especially regarding the possibility of roughness at the 7.16 m gage, but no definite cause was determined.

Comparison of Re_T in Fig. 1 with data from Ref. 1 indicates that the largest values from the present data[4] are more than double those reported in Ref. 1 for similar wall cooling ratios. This finding prompted further experimentation over a range of M_s. For these tests p_1 was held at 2.933 kPa. Thus Re_u varied inversely with T_w/T_e. The data are presented in Fig. 2 with only the largest Re_T value from the gage locations being shown. Included in the figure are data from Refs. 3, 5, and 6 along with the proposed transition reversal curves for $Re_u = 1.6 \times 10^6$/m from Ref. 3.

Observe in Fig. 2 that the present Re_T are significantly larger than the referenced data, except for Ref. 6 at $T_w/T_e < 0.3$. Since the gas-dynamic conditions were similar for the data shown, explanations for the larger Re_T point toward facility differences. Possibly the larger transverse tube dimension for the present study (12.7 cm) was responsible for the higher Re_T compared to Refs. 3 and 5 where the shock tubes were 10.16 cm diam and 3.81×6.85 cm, respectively. This trend of higher Re_T with increasing tube size was given theoretical support by Boehman[2] who showed experimental evidence by comparing data from Refs. 3 and 6 as in Fig. 2 where the Ref. 6 data are seen to be higher. The shock tube in Ref. 6 was 43.18 cm in diameter. These comparisons of results from different size facilities, however, do not provide firm support of the proposed trend. For example, from Fig. 2 consider the magnitude of increase in Re_T ratioed to the increase in transverse dimension. This sensitivity ratio calculated from comparison of the present data with Refs. 3 or 5 is not consistent with the ratio derived from comparison of Refs. 3 and 6. Also, the trend with transverse dimension is reversed when comparing Ref. 6 to the present data for $T_w/T_e > 0.3$, but there could be an Re_u effect in this case. As a result, it cannot be concluded that shock-tube size alone was responsible for the higher Re_T in the present investigation. Probably there were interacting effects of Re_u, M_s, shock tube configuration, and undefined disturbances which contributed to these results.

Another observation from Fig. 2 is that transition reversal occurs at $T_w/T_e \approx \frac{1}{3}$ for both Ref. 3 and the present data. This result is particularly interesting when consideration is given to the differences in Re_u, Re_T, and shock-tube configurations. Reference 6 data also indicate a change in the Re_T trend at the same level of wall cooling, although the change is not an abrupt reversal. These results tend to support Boehman's[2] calculations wherein certain solutions to the parallel flow stability equations exhibit a "changeover Reynolds number" phenomenon which may be associated with transition reversal. However, further experimental and theoretical work is required to identify and study the parameters controlling this phenomenon in order to aid understanding of reversal for the full range of wall cooling.

References

[1] Ostrach, S. and Thornton, P.R., "Stability of Compressible Boundary Layers Induced by a Moving Wave," *Journal of the Aerospace Sciences*, Vol. 29, March 1962, pp. 289-296.

[2] Boehman, L.I., "The Stability of Highly Cooled Compressible Laminar Boundary Layers," AFFDL-TR-76-148, Oct. 1976.

[3] Boison, J.C., "Investigation of Test Facility Environmental Factors Affecting Boundary Layer Transition," AFFDL-TR-73-106, Sept. 1973.

[4] Chaney, M.J., "Effect of Driver-Created Disburbances on Shock Tube Sidewall Boundary-Layer Transition," MS Thesis, Iowa State University, Ames, 1977.

[5] Hartunian, R., Russo, A., and Marrone, P., "Boundary-Layer Transition and Heat Transfer in Shock Tubes," *Journal of the Aerospace Sciences*, Vol. 27, Aug. 1960, pp. 587-594.

[6] Golobic, R.A., "Measurements of Boundary Layer Transition on a Shock Tube Wall for Wall Cooling Ratios Between 0.39 and 0.225," Frank J. Seiler Research Laboratory, U.S. Air Force Academy, Colorado Springs, Colo., Rept. SRL-TR-75-0022 (AD A021406), Dec. 1975.

Derivation of the Fundamental Equation of Sound Generated by Moving Aerodynamic Surfaces

Hans R. Aggarwal*
University of Santa Clara, Santa Clara, California

THE fundamental equation of sound generated by arbitrarily moving aerodynamic surfaces was first derived by Ffowcs Williams and Hawkings.[1] These authors based their derivation on the study of mass and momentum balance of a control volume imbedding a mathematical surface(s) exactly corresponding to the real surface(s). They also sketched an alternative method, employing generalized functions, for its derivation. The latter method, later developed by Farassat,[2] is purely mathematical and formal. Yet another, implicit, derivation of the Ffowcs Williams and Hawkings equation was given by Goldstein[3] through the use of free-space Green's function. This Note generalizes Lowson's[4] concept of moving point singularities to moving surface singularities and gives a new derivation of the fundamental equation. The present derivation is based on topological considerations of the underlying space, the fluid medium, and the integral properties of the Dirac delta function. It is simple, direct, physical, and instructive.

For a fluid medium containing arbitrarily moving point mass and force singularities, the equations of continuity and momentum, in their conservation form, may be written as[4]

Received Oct. 25, 1982; revision received Dec. 20, 1982.

*Senior Research Associate, Department of Mechanical Engineering.